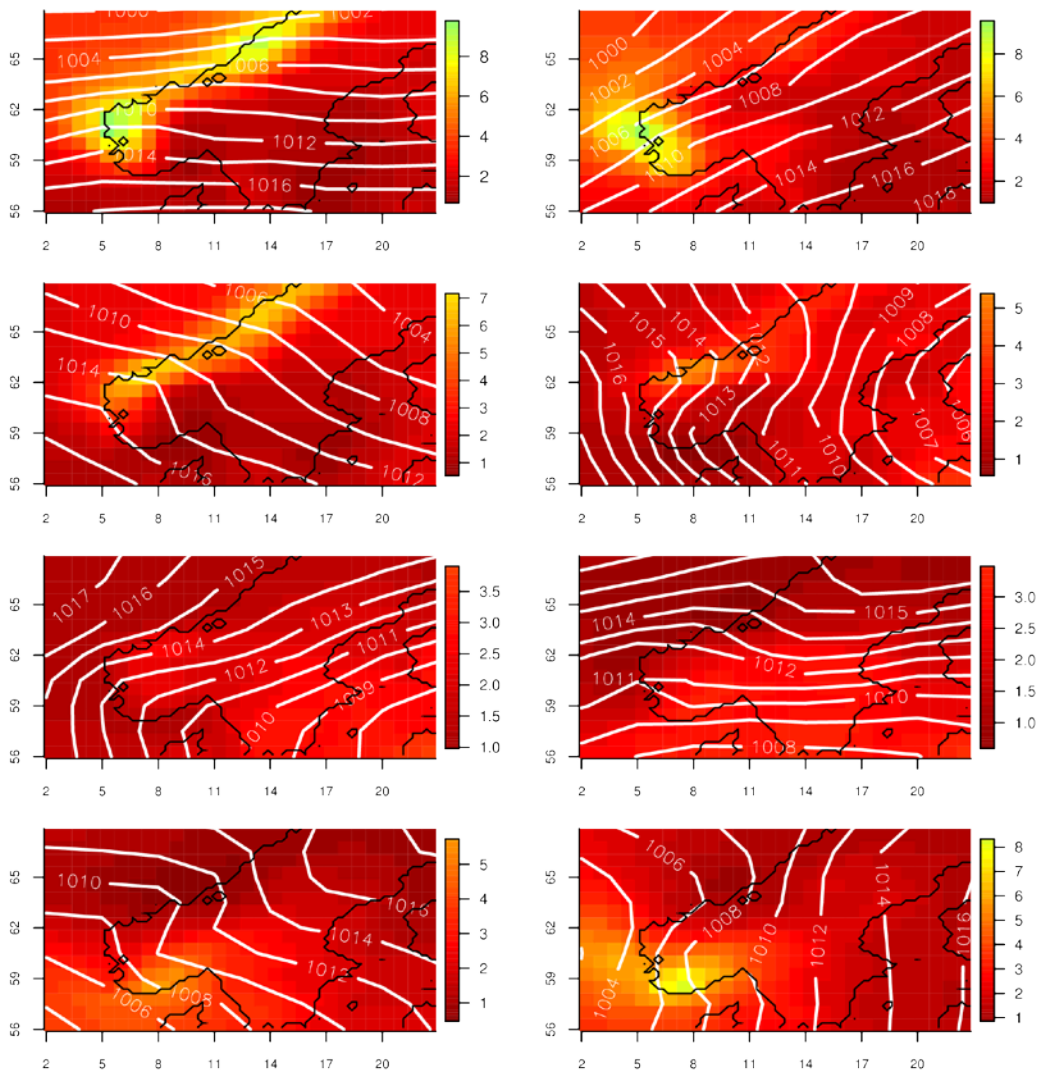




# Evaluation of circulation patterns over Scandinavia from ENSEMBLES regional climate models

Oskar A. Landgren, Torill Engen Skaugen, Jan Erik Haugen



**Eight pressure patterns based on daily mean sea-level pressure from ERA-Interim data 1981-2000 using Grosswetterlagen classification. The mean daily precipitation [mm/day] corresponding to each class is shown as the color map below the MSLP contour lines.**

Postal address  
P.O.Box 43, Blindern  
NO-0313 OSLO  
Norway

Office  
Niels Henrik Abelsvei 40

Telephone  
+47 22 96 30 00

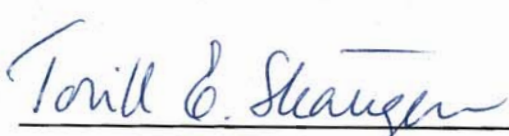
Telefax  
+47 22 96 30 50

e-mail: [met@met.no](mailto:met@met.no)  
Internet: [met.no](http://met.no)

Bank account  
7694 05 00628

Swift code  
DNBANOKK



<b>Title</b> Evaluation of circulation patterns over Scandinavia from ENSEMBLES regional climate models	<b>Date</b> April 30th 2013
<b>Section</b> Model and Climate analysis	<b>Report no.</b> no. 4/2013
<b>Author(s)</b> Oskar A. Landgren, Torill Engen Skaugen, Jan Erik Haugen	<b>Classification</b> <input checked="" type="checkbox"/> Free <input type="checkbox"/> Restricted
	ISSN 1503-8025
	e-ISSN 1503-8025
<b>Client(s)</b> Statkraft, The Norwegian Meteorological Institute	<b>Client's reference</b> MIST-1
<b>Abstract</b> <p>The performance of regional climate models (RCMs) over Scandinavia is dependent on their representation of the atmospheric circulation patterns. In order to assess the quality of this representation, we here conduct a study comparing different circulation type classes (representative pressure patterns), their annual cycle of occurrence as well as evolution in occurrence over time in the models. Daily mean sea-level pressure (MSLP) from RCM runs from the ENSEMBLES project in 25 km resolution is used. 6-hour MSLP data from ECMWF Interim re-analysis (ERA-Int) is averaged over 24 hours and used as reference. RCM and ERA-Int data is bi-linearly interpolated to the domain defined by 2-23° longitude, 56-68° latitude, in 3°×1.5° resolution, yielding 8×9=72 points on a rectangular grid. The time period of study is 1981-2000. Different classification methods from the EU COST Action 733 cost733class software are used to define circulation type classes from ERA-Int. The circulation type classes are then applied to the RCM runs. The mean monthly representation of the circulation type classes is presented and compared between ERA-Int and the RCMs. The results show that particularly one model run, DMI-HIRHAM5-ECHAM5 is deviating strongly from the others. DMI-HIRHAM5-ARPEGE and METNO-HIRHAM-BCM are also misrepresenting some circulation classes. Two classification methods, Simulated ANnealing and Diversified RANdomization (SANDRA) and Self-Organizing Maps (SOM), produce similar classes, while most other produce rather different classes. The methods by Lund and Kirchofer as well as P XK (PCA-based extreme-score with k-means clustering) did not manage to produce classes from ERA-Int that were applicable to the RCM runs. For all methods except Grosswetterlagen (which is based on pre-defined classes) a higher number of classes seems to increase the risk of mismatching.</p> <p>In addition, the number of annual occurrences of the circulation type classes in each model was also plotted for the simulated future period until year 2100. Most models show change in occurrence within ±10% compared to 1981-2000, but ARPEGE-based models show a larger increase in high-pressure occurrence over the centre part of the domain.</p>	
<b>Keywords</b> Circulation types, RCM, ENSEMBLES, Scandinavia	
<b>Project leader</b>   <hr/> <b>Torill Engen Skaugen</b>	<b>Responsible signature</b>   <hr/> <b>Øystein Hov</b>

## 1. Introduction

Norway typically experiences warm moist air from the south-western parts of the Atlantic Ocean. The high mountain regions further inland lead to large annual precipitation amounts in western parts of the country. One of the challenges in climate modelling is the representation of the hydrological cycle and the atmospheric circulation patterns experienced in Scandinavia. How trustworthy are the precipitation projection available for this region? And how is the atmospheric circulation projected to change in the future?

Over almost the same region as in Landgren et al. (2012), Tveito (2010) compared classification methods given by the EU COST Action 733 project<sup>1</sup>. The project produced a catalogue<sup>2</sup> (Philipp et al. 2010) with 27 different methods in different setups, totalling 73 different classification catalogues based on different parameters (e.g. MSLP, Z500, Z850, U/V 700) from the ERA-40 dataset (Uppala et al. 2005). Tveito (2010) compared the classifications against data from four meteorological stations in Norway. The method used here is partly based on his conclusions. Huth et al. (2008) provides a review of the advances within the field up until the COST733 action, including differences in approaches (manual, hybrid and automated), introduction of principal component analysis (PCA), cluster analysis, nonlinear methods and optimisation algorithms.

Different studies analyses the circulation patterns by using circulation type classification, covering all or parts of Scandinavia, e.g. Chen (2000), Lindersson (2001). Many studies have also attempted to explain various events using circulation type classification, including winter temperatures (Chen 2000, Tveito 2007) and hydrological drought (Fleig et al. 2010).

The advance of climate models has paved the way for studying trends in the realisation of circulation patterns, e.g. Huth (2000, 2001). Plavcová & Kysely (2013) conducted a study using a subset of the same regional climate model (RCM) data as presented here by applying a classification method using 11 predefined circulation types. They found the change in the occurrence frequency during the 21<sup>st</sup> century to be largest for runs based on the BCM GCM (Furevik et al. 2003); from -6% for the spring southerly winds to +8% for winter westerly winds.

A study on weather type conditions is here performed on the precipitation projections obtained by the ENSEMBLES project<sup>3</sup> on the historical (control) runs in an attempt to reveal their reliability. Do the models fail to represent the atmospheric circulation patterns? The projected change in circulation types is then estimated.

An evaluation of the ENSEMBLES RCM runs covering Scandinavia is performed by Landgren et al. (2012). They found that some model runs were clear outliers in terms of especially representation of the annual precipitation cycle. The ERA-Interim dataset (Dee et al. 2011) is used as a reference dataset in order to derive the most common atmospheric

---

<sup>1</sup> <http://cost733.met.no/>

<sup>2</sup> <http://geo23.geo.uni-augsburg.de/cost733wiki/Cost733Cat2.0>

<sup>3</sup> <http://ensemblesrt3.dmi.dk/>

circulation patterns that represent the different weather types over Scandinavia. The classes (patterns) are compared to the modelled datasets to reveal how well they agree.

Despite the tempting idea to use as many parameters as possible to obtain a better classification, some constraints were imposed by the sheer amount of data<sup>4</sup>. Since the aim of this study was to set up a simple experiment to compare performance of different models, the single parameter finally used was mean sea-level pressure (MSLP or PSL) in time resolution of daily mean values.

The reanalysis and model data used is presented in Section 2. The methods are described in Section 3. The results are presented in Section 4, a discussion is given in Section 5 and summary and concluding remarks are presented in Section 6.

## 2. Data

Data from the re-analysis dataset ERA-Interim (Section 2.1) and the ENSEMBLES RCM runs (Section 2.2) were used in the present study. Different re-analyses and observational based datasets were available for comparison, including the ERA-40 (Uppala et al. 2005), the E-OBS dataset (Van den Besselaar et al. 2011). The ERA-Interim reanalysis was used due to higher resolution compared to ERA-40. The E-OBS dataset could not be used as it does not cover ocean areas. The hindcast dataset NORA10 produced at the Norwegian Meteorological Institute could have been used, but was stored on a rotated grid and not available in NetCDF format.

### 2.1 ERA-Interim reanalysis

Pressure fields from the ERA-Interim reanalysis (Dee et al. 2011) are used as reference data for establishing the classes. The data was downloaded from [http://data-portal.ecmwf.int/data/d/interim\\_full\\_daily](http://data-portal.ecmwf.int/data/d/interim_full_daily) in time resolution of six hours on the native  $0.75^{\circ} \times 0.75^{\circ}$  grid.

---

<sup>4</sup> The daily MSLP data for the ENSEMBLES RCM runs required downloading about 110 GB.

## 2.2 Regional Climate Model runs

The ENSEMBLES project's RCM runs over Europe are used. The model runs used are presented in Table 2.1.

Country	Institute	RCM	GCM providing boundary conditions
Ireland	C4I	RCA3	ECHAM5
		RCA3	HadCM3Q16
France	CNRM	RM4.5	ARPEGE
		RM5.1	ARPEGE
Denmark	DMI	HIRHAM	ARPEGE
		HIRHAM	BCM
		HIRHAM	ECHAM5
Switzerland	ETHZ	CLM	HadCM3Q0
Germany	GKSS	CLM	IPSL
UK	HC	HadRM3Q0	HadCM3Q0
		HadRM3Q3	HadCM3Q3
		HadRM3Q16	HadCM3Q16
Italy	ICTP	RegCM	ECHAM5
Netherlands	KNMI	RACMO	ECHAM5
		RACMO	MIROC3.2-hires
Norway	METNO	HIRHAM	BCM
		HIRHAM	HadCM3Q0
Germany	MPI	REMO	ECHAM5
Canada	OURANOS	CRCM	CGCM3
Sweden	SMHI	RCA	BCM
		RCA	ECHAM5
		RCA	HadCM3Q3
Spain	UCLM	PROMES	HadCM3Q0
Russia	VMGO	RRCM	HadCM3Q0

Table 2.1: RCM runs used in the present study. The name of the RCM, the driving GCMs as well as the institute running them and the country they are located in are listed in the Table. As shown in the Table, some RCMs are run with multiple GCMs.

A few models were not included due to technical reasons:

- DMI-HIRHAM5-BCM and GKSS-CCLM-IPSL runs were on coordinate formats incompatible with the preparation tool used (CDO, Climate Data Operators).
- UCLM-PROMES-HadCM3Q0 could not be implemented due to an unknown error in the classification which returned just 6 classes instead of 9.
- VMGO-RRCM-HadCM3Q0 data was offline at the moment of the study.

The model runs are available from the RCM data portal at <http://www.ensemblesrt3.dmi.dk> (RCM data portal → RT2B, Transient experiments driven by global experiments).

### 3. Method

The ERA-Interim and ENSEMBLES RCM data was interpolated to a common 3x1.5-degree grid (2-23° lon, 56-68° lat, shown in Fig. 3.1). Note that this domain differs in resolution as well as slightly in geographical extent from the domain used in Landgren et al. (2012). This was because the classification tool did not support missing values, which was the case for some models north of approximately 69 degrees latitude. The latitude resolution of 1.5 degrees was chosen as it gave roughly the same distance in kilometres between the grid points as the 3.0 degrees longitude resolution. The whole domain then gave  $8 \times 9 = 72$  points.

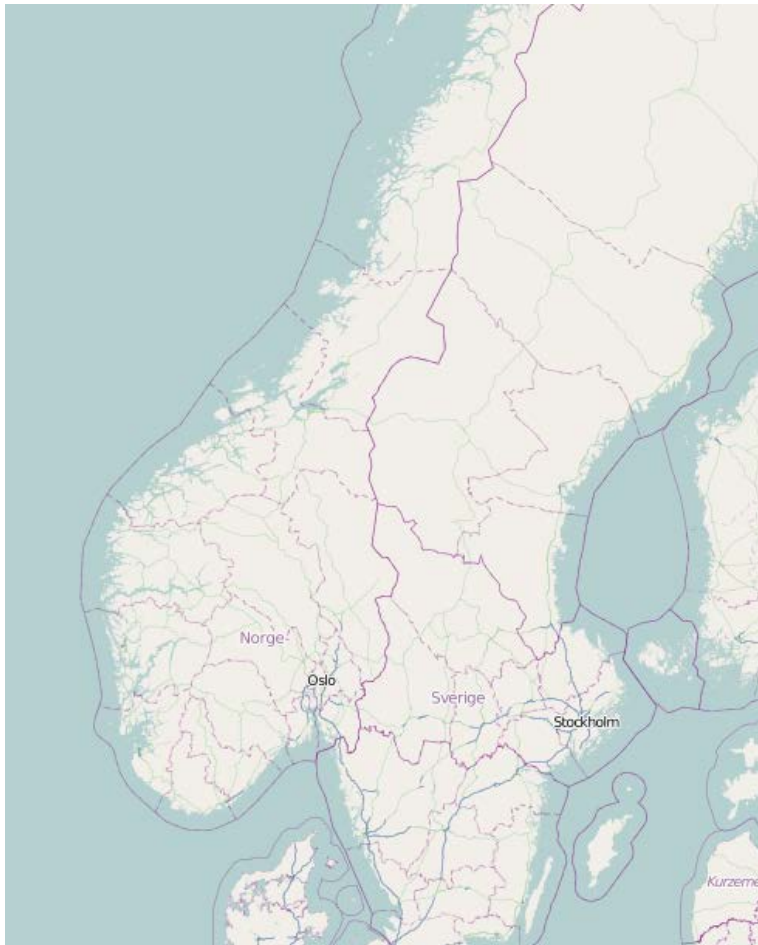


Fig. 3.1: The region used in this study; 2-23° longitude, 56-68° latitude, covering most of Scandinavia. Map © OpenStreetMap contributors.

A reference period of the years 1981-2000 was chosen since it is covered by ERA-Interim (Dee et al. 2011) (1979-present) and is within the historical period (20C3M<sup>5</sup>) of the RCM runs (1900-2000).

The classification framework *cost733class*<sup>6</sup> from the EU COST action 733 was used as it includes many different methods of the leading science in the field in a single software package. 6 different methods were chosen that could handle approximately 10 atmospheric

<sup>5</sup> 20th Century Climate in Coupled Models, <http://www.ipcc-data.org/ar4/scenario-20C3M.html>

<sup>6</sup> <http://cost733class.geo.uni-augsburg.de/cost733class-1.2>

circulation type classes and that only required mean sea level pressure (MSLP). In order to use the MSLP-fields with the `cost733class` methods, the data was first converted to text files in a tab-separated text format in R<sup>7</sup>. The ERA-Interim dataset was then divided in atmospheric circulation type classes, by using the methods presented below.

The different weather type classification methods and number of classes used are listed in Table 3.1.

Method in <code>cost733class</code>	Number of classes used
GWT – Grosswetterlagen	8, 10, 18, 27
KIR – Kirchofer	9
LND – Lund	9
PXK – PCA extreme score with k-means clustering	8, 12
SANDRA – Simulated annealing and diversified randomization	5, 6, 7, 8, 9, 18, 27
SOM – Self-organizing maps	5, 6, 7, 8, 9

Table 3.1: Classification methods used in the present study.

*Grosswetterlagen* (Beck et al. 2007), is based on pre-defined types, e.g. for 8 classes the main wind directions become N, NE, E, SE, S, SW, W and NW. Higher numbers add combinations with cyclonic or anticyclonic patterns. The other methods generate the classes using different numerical methods.

*Lund* (1963) is based on a leader algorithm, which means that all observations (the MSLP field over the whole region for one point in time constitutes one observation) are compared to each other using the correlation coefficient. The observation with the highest number of similar cases (using a default threshold value of 0.7) is declared the leader of the first class and all of the observations similar are assigned to this class. They are then removed and the process is repeated until the desired number of classes has been found. Finally all observations are put back and assigned to the most similar leader. *Kirchofer* (Kirchhofer 1974, Blair 1998) modified this method by using correlation for each column (longitude) and row (latitude), thus making sure that the patterns are similar in all parts of the map.

*PXK* is based on Principal Component Analysis (PCA) to determine the initial classes and an extreme score method (Esteban et al. 2006, Philipp et al. 2010) to evaluate the classes before a k-means clustering process takes place. There the average of all observations belonging to each class is calculated and then all observations are assigned to the most similar of the class averages. The k-means process is repeated until convergence.

*Simulated annealing and diversified randomization* (Philipp et al. 2007) is based on k-means clustering but attempts to avoid local optima by a probability of re-assigning observations to random classes. This probability decreases as the method progresses. The method is rather quick, so in order to improve the chances of finding the global optimum the method starts over with randomly assigned starting positions and assignments a user-selectable number of times. The final result is then selected as the collection of classes with the highest within-type variance.

<sup>7</sup> <http://www.r-project.org>

*Self-organising maps* (Kohonen 1990) uses classes with initially random values. The observations are assigned to the closest class using Euclidian distance measure and then the classes are modified using a weighted mean of the observation. The classes are connected in a one-dimensional neural network so that the changes to one class affect the neighbours on each side.

For the methods SANDRA and SOM, the number of runs has to be specified. For this particular study, attempts with more runs only improved the Explained Cluster Variance value marginally (e.g. for SANDRA with 9 classes, the ECV value increased from 0.805398 to 0.805454 with a 20-fold increase from 100 to 2000 runs) and showed no visible difference in the classes produced. 100 runs were therefore considered enough.

When the classification process had been carried out on the ERA-Interim dataset, the resulting patterns (classes) were applied to each RCM run. This was done using the cost733class method ASC (assign), where each day in the RCM runs are assigned to the closest class measured by the default (Euclidean) distance measure. Each point in the area is considered and the day is assigned to the class with the smallest overall difference.

The time series of dates and associated classes could then be analysed. As climate models develop their own climatology we cannot always expect a circulation pattern for a certain point in time in one model to be closely related to a pattern from observation data for that time. In order to compare results from different RCMs the annual distribution for each class was determined for the years 1981-2000.

In addition to evaluating the RCM results against the ERA-Interim dataset, a future outlook of the RCMs was performed. The number of annual occurrences of each class were determined for each year in the period 1981-2100 (where available) to investigate if there were any long term trends in the simulations.

More details and references on the methods are available in the cost733class-1.2 User guide<sup>8</sup> and in Philipp et al. (2010).

## 4. Results

Different classification methods were performed on the ERA Interim dataset as described in Section 3. The results show that different classification methods provide different results. However, some methods also showed similar results.

In order to highlight two methods with fundamentally different approaches and different results, we have chosen to present results from the methods GWT08 (Grosswetterlagen with 8 classes) and SAN06 (SANDRA with 6 classes). These numbers of classes were chosen as additional classes added were similar to the ones already produced. Examples of results from methods using higher number of classes are presented in the Appendix; Figs. A.1-A.2 for GWT with 26 classes and Figs. A.3-A.4 for SANDRA with 27 classes. An example of results

---

<sup>8</sup> [http://cost733class.geo.uni-augsburg.de/cost733class-1.2/export/HEAD/doc/cost733class\\_userguide.pdf](http://cost733class.geo.uni-augsburg.de/cost733class-1.2/export/HEAD/doc/cost733class_userguide.pdf)

from SOM, similar to those from SANDRA, is presented in Figs. A.5-A.6. Results from the methods Lund, Kirchofer and P XK are presented in Figs. A.7-A.12.

#### 4.1 Circulation type classification

The circulation patterns retrieved from weather type classification of ERA-Interim for the period 1981-2000 are shown for GWT08 and SAN06 in Fig. 4.1a and 4.1 b respectively. To show the precipitation impact, the mean precipitation for each of the classes was calculated using ERA-Interim precipitation from the days assigned to each class.

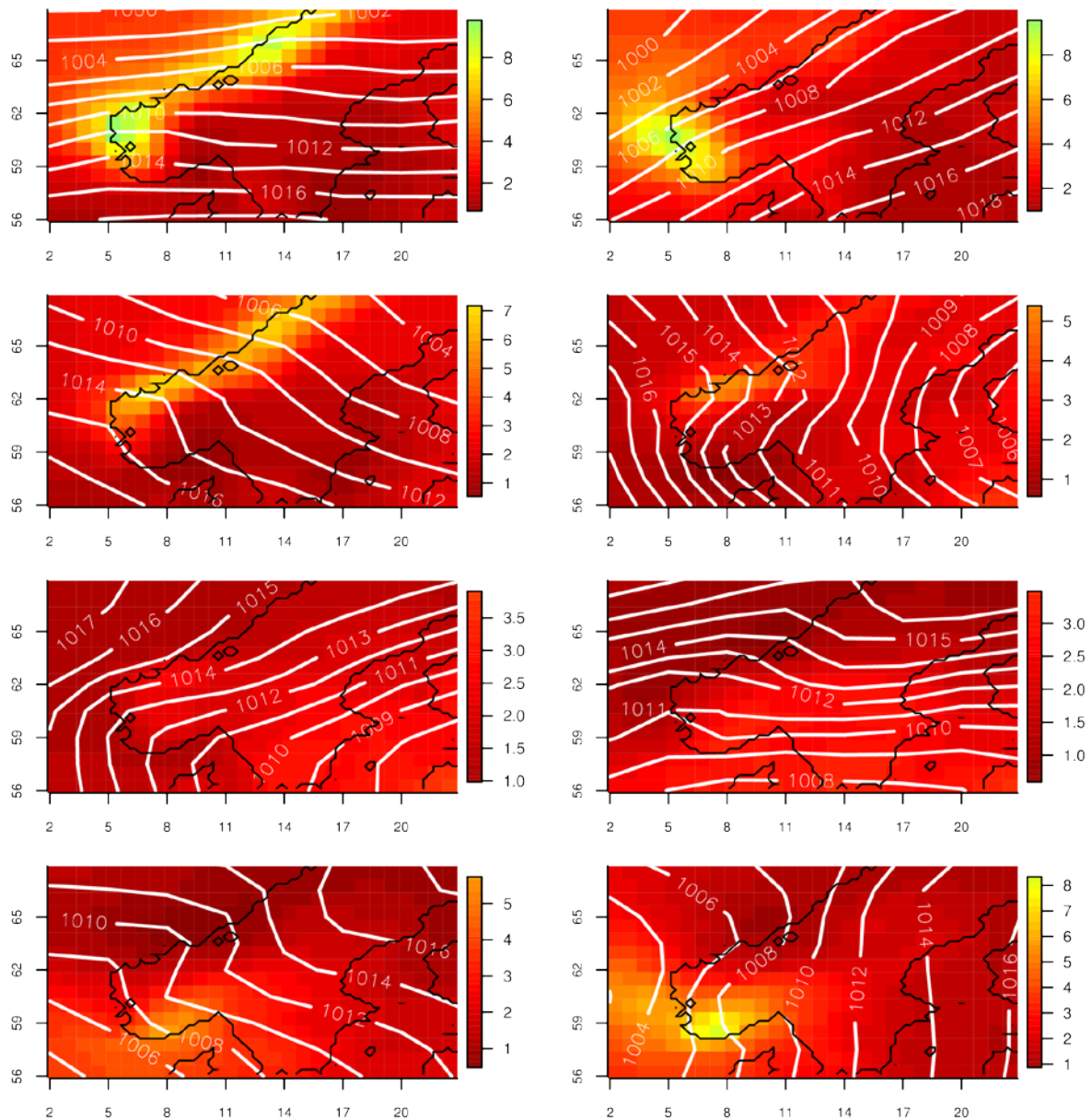


Fig. 4.1a: Pressure classes from ERA-Interim MSLP based on the Grosswetterlagen method with 8 classes (GWT08). The pressure fields are shown as contour lines. The underlying colour maps show the mean daily precipitation [mm/day] in ERA-Interim for the days belonging to each class.

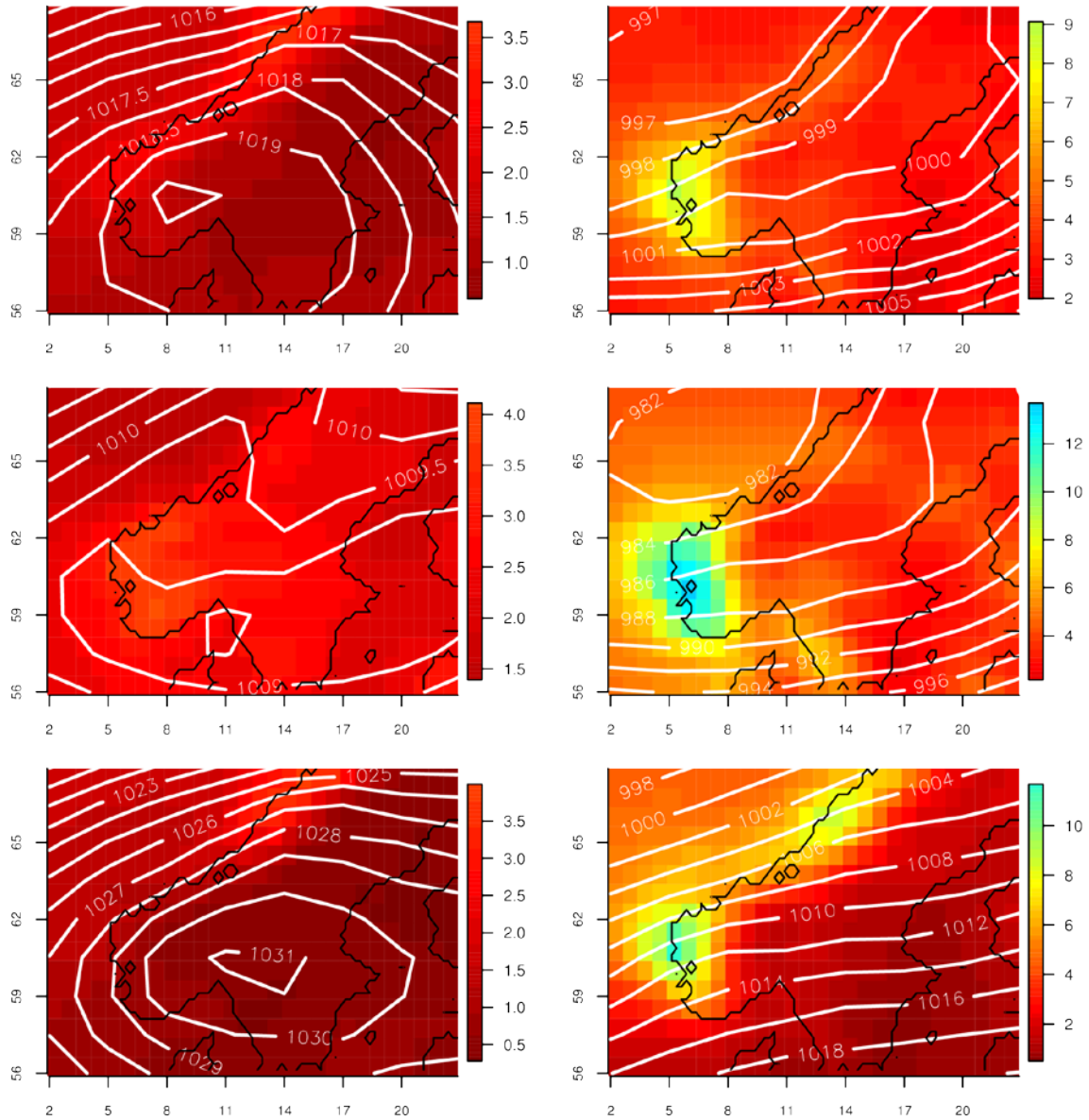


Fig. 4.1b: Pressure classes from ERA-Interim MSLP derived using the SANDRA method with 6 classes (SAN06). The pressure fields are shown as contour lines. The underlying colour maps show the mean daily precipitation [mm/day] in ERA-Interim for the days belonging to each class.

## 4.2 Annual distribution

The annual distribution of the classes retrieved in Section 4.1 is here presented. The mean number of days per month for the period 1981-2000 is plotted on the y axis against month on the x axis. The results are shown for GWT08 in Fig. 4.2a and SAN06 in Fig. 4.2b.

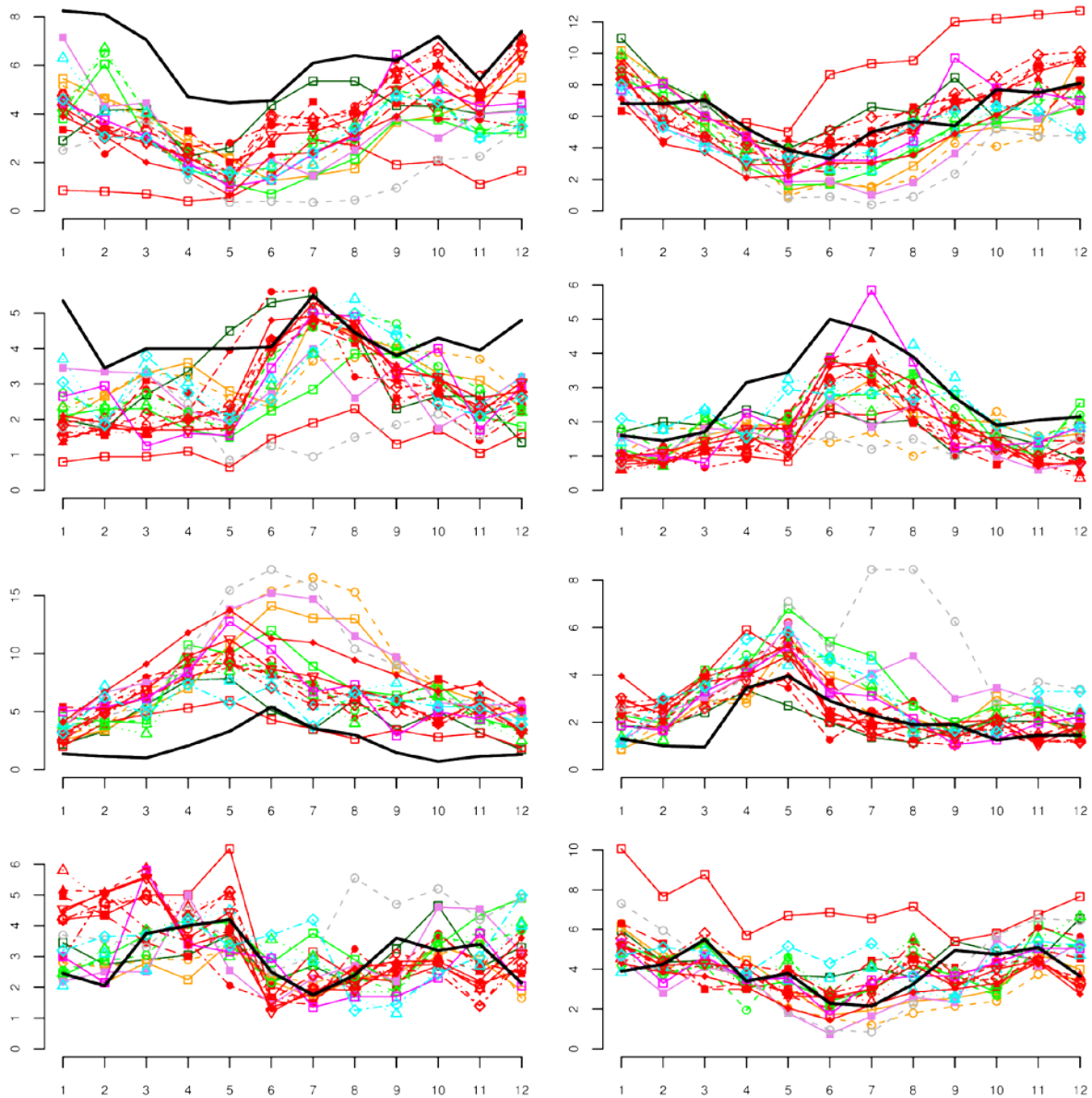


Fig. 4.2a: The annual distribution of the different classes for GWT08. Each of the eight charts corresponds to the classes in Fig. 4.1a. On the x-axis are the different months (1-12 meaning January-December). The y-axis shows the number of days per month classified as the respective classes. ERA-Interim is shown in black. Legend is presented in Fig. 4.3.

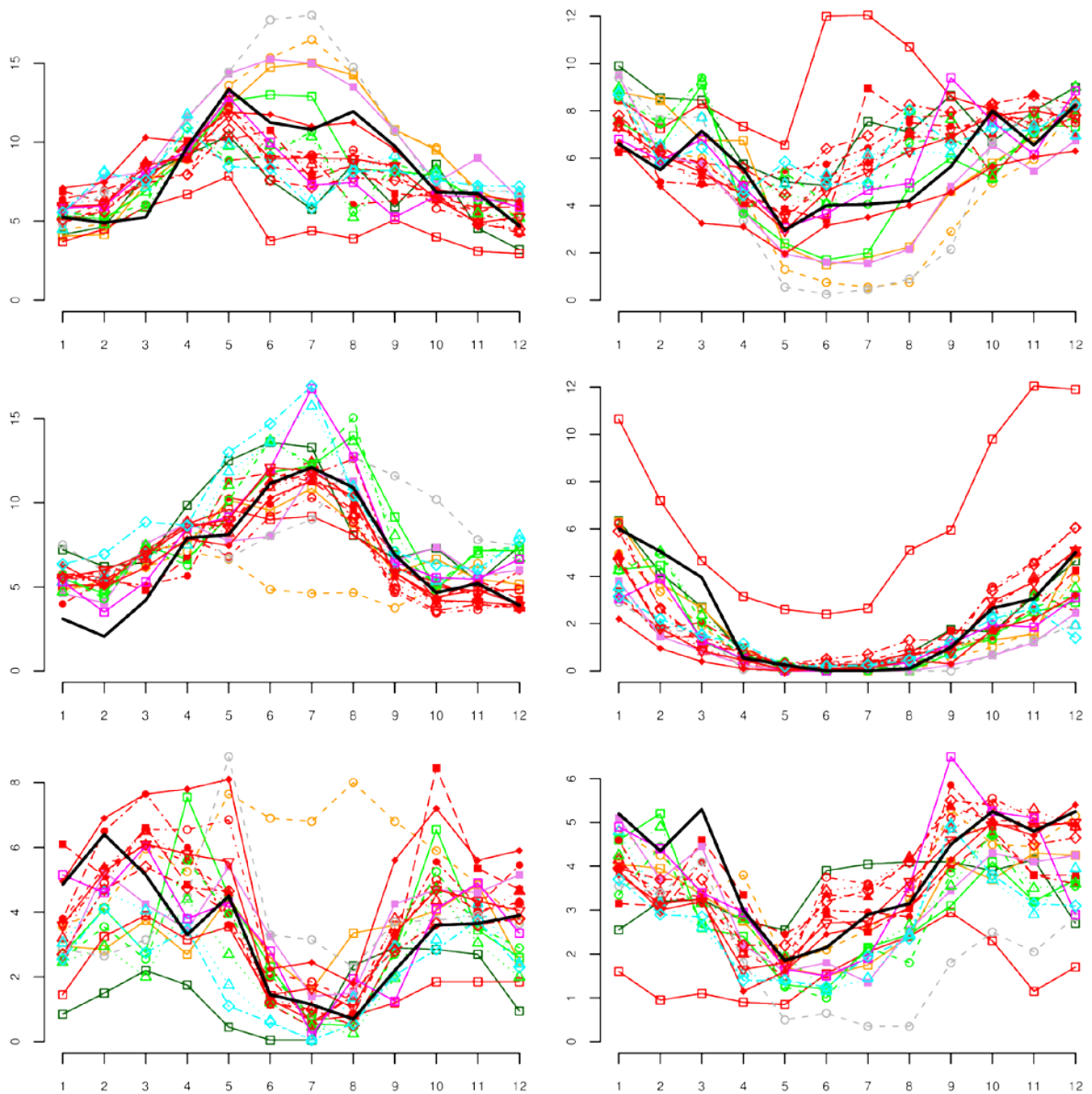


Fig. 4.2b: The annual distribution of the different classes for SAN06. Each of the six charts correspond to the classes in Fig. 4.1b. On the x-axis are the different months (1-12 meaning January-December). The y-axis shows the number of days per month classified as the respective classes. ERA-Interim is shown in black. Legend is presented in Fig. 4.3.

- ERA-Interim
- C4IRCA3\_A1B\_HadCM3Q16\_DM\_25km
- CNRM-RM5.1\_SCN\_ARPEGE\_DM\_25km
- DMI-HIRHAM5\_A1B\_ARPEGE\_DM\_25km
- DMI-HIRHAM5\_A1B\_ECHAM5\_DM\_25km
- ETHZ-CLM\_SCN\_HadCM3Q0\_DM\_25km
- ICTP-REGCM3\_A1B\_ECHAM5\_r3\_DM\_25km
- KNMI-RACMO2\_A1B\_ECHAM5-r1\_DM\_50km
- KNMI-RACMO2\_A1B\_ECHAM5-r2\_DM\_50km
- KNMI-RACMO2\_A1B\_ECHAM5-r3\_DM\_25km
- KNMI-RACMO2\_A1B\_ECHAM5-r3\_DM\_50km
- KNMI-RACMO2\_A1B\_MIROC3.2-hires\_DM\_50km
- METNOHIRHAM\_SRESA1B\_BCM\_DM\_25km
- METNOHIRHAM\_SRESA1B\_HadCM3Q0\_DM\_25km
- METO-HC\_HadRM3Q0\_A1B\_HadCM3Q0\_DM\_25km
- METO-HC\_HadRM3Q3\_A1B\_HadCM3Q3\_DM\_25km
- MPI-M-REMO\_SCN\_ECHAM5\_DM\_25km
- OURANOSMRCC4.2.1\_A1B\_CGCM3\_DM\_25km-CRU
- SMHIRCA\_A1B\_ECHAM5\_DM\_50km
- SMHIRCA\_A1B\_ECHAM5-r3\_DM\_25km
- SMHIRCA\_A1B\_HadCM3Q3\_DM\_25km

Fig. 4.3: Legend for Figs. 4.2 and 4.4.

### 4.3 Future estimates

The annual occurrence of each class was plotted for the time interval 1981-2100.

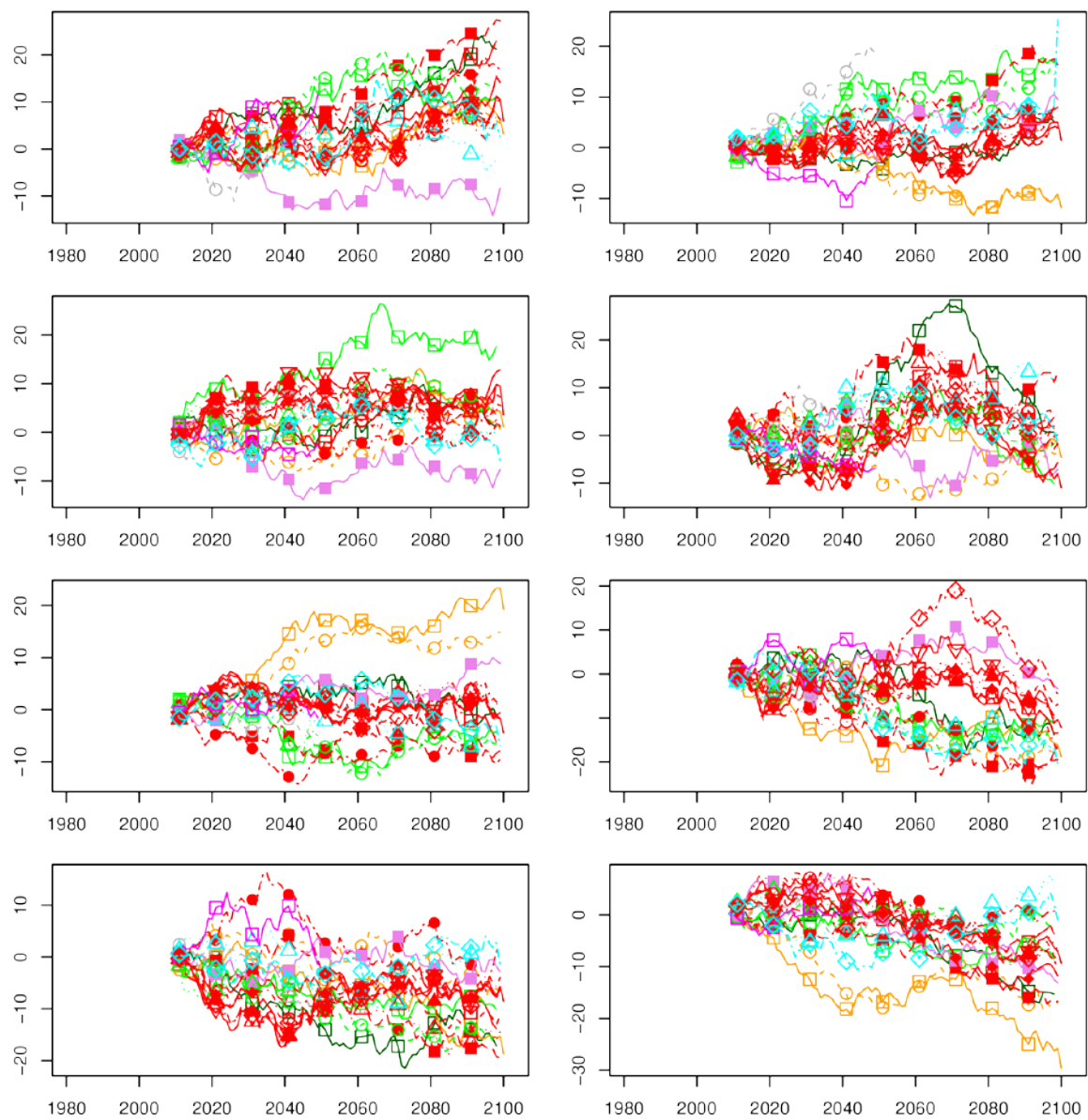


Fig. 4.4a: Timeline for GWT08 showing the relative change in yearly occurrence (y-axis, in percent change) of each class classified as each of the eight classes in 4.1a. The data has been smoothed using a 30-year moving average.

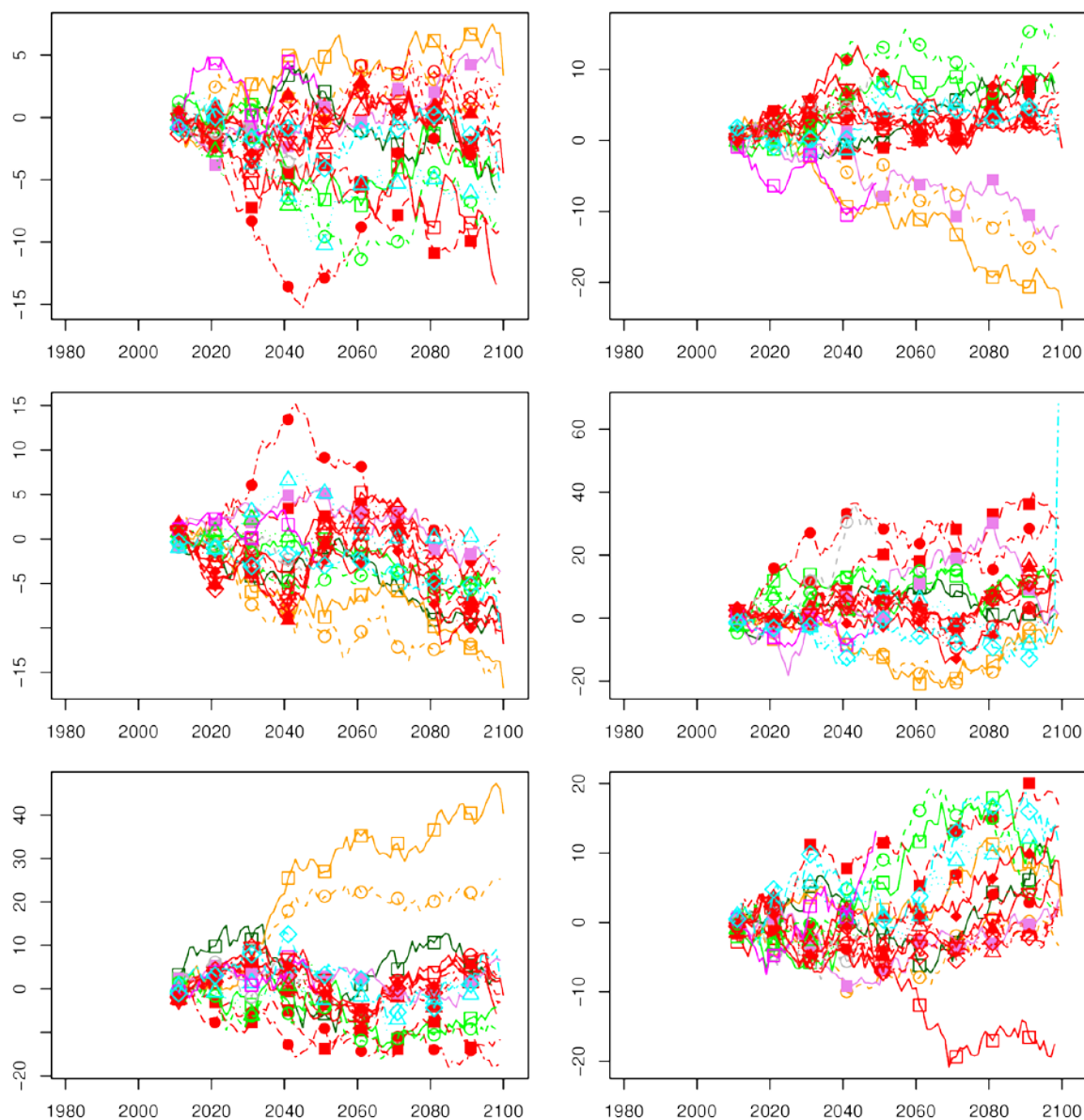


Fig. 4.4b: Timeline for SAN06 showing the relative change in yearly occurrence (y-axis, in percent change) of each class classified as each of the six classes in 4.1b. The data has been smoothed using a 30-year moving average.

## 5. Discussion

The classes of two of the methods (GWT08 and SAN06) are presented in Fig. 4.1a and 4.1b respectively. Of the different methods tried, only a few could provide classes from training with ERA-Interim that also represented the RCM runs. The methods Lund (Figs. A.7-8), Kirchofer (Figs. A.9-10) and PXX (Figs. A.11-12) all gave very different annual cycle for the RCMs compared to ERA-Interim. This could be interpreted as a difference between ERA-Interim and the ENSEMBLES RCMs. Perhaps if the models were spread more on both sides of ERA-Interim this could be more justified, but it seems unlikely that the RCM results would be as grouped together that far away from ERA-Interim. This difference is also found, although to a smaller extent, for classifications made with Grosswetterlagen method using higher number of classes (Fig. A.1-2).

Also, it was clear that all methods except Grosswetterlagen tended to produce collections where some classes within the same collection were very similar. This can lead to increasing mismatch for higher number of classes. This was a problem for all methods except Grosswetterlagen, which uses pre-defined differentiated classes (Fig. A.1), although all of those classes are not always representative of the patterns in the region. SANDRA and SOM produce very similar results, at least for number of classes below 10, with an example shown in Figs. A.5-A.6.

The results indicate that one model, DMI-HIRHAM5-ECHAM5, is a strong outlier when comparing the annual distribution of circulation types (Fig. 4.2). Comparing with the findings in Landgren et al. (2012), this may be part of the reason why it shows an overestimation of precipitation in Oslo (A.2a) and Östersund (A.10a) and an underestimation in the winter for Bergen (A.4a) and Trondheim-Værnes (A.6a). Another frequent outlier from the same study however, MPI-M-REMO-ECHAM5 run however does not show up as significantly different from the rest here. A third model which could be of interest is VMGO-RRCM-HadCM3Q0 which was ranked worst in that study but could not be retrieved at the time of this study.

Other models not following the rest in terms of annual distribution are: DMI-HIRHAM5-ARPEGE and METNO-HIRHAM-BCM. Many other models follow the ERA-Interim distribution of patterns quite well.

The time evolution in Fig. 4.4 indicates that the occurrence of most classes does not change much, as most models stay within a  $\pm 10\%$  interval. Some grouping can be revealed however, with the model runs driven using on ARPEGE as boundary conditions produce more high-pressure systems over the centre of the domain in the latter part of the 21<sup>st</sup> century (Fig. 4.4b, the bottom left class). This trend could also be seen in GWT10, GWT26 and SAN27 where a similar class was present. For the other models however, there is a lot of variations in the results, but probably something for a future study.

## 6. Conclusion

Circulation type classification may provide valuable information when comparing the performance of different models. Although very simple, this study highlights one model run, DMI-HIRHAM5-ECHAM5, as a clear outlier in terms of circulation patterns compared to the rest of the model ensemble. Additional studies should be made in order to perform a more thorough analysis and to include more parameters.

## Acknowledgements

The authors would like to thank Ole Einar Tveito and Jean-Marie Lepioufle for valuable discussions. The present report was funded within the “MIST-klimaprojeksjoner prosjekt”, a collaboration project between Statkraft and the Norwegian Meteorological Institute. The ENSEMBLES data used in this work was funded by the EU FP6 Integrated Project ENSEMBLES (Contract number 505539), whose support is gratefully acknowledged.

## References

- Beck, C., Jacobeit, J., & Jones, P. D. (2007). Frequency and within-type variations of large-scale circulation types and their effects on low-frequency climate variability in central Europe since 1780. *International journal of climatology*, 27(4), 473-491.
- Van den Besselaar, E. J. M., Haylock, M. R., Van der Schrier, G., & Klein Tank, A. M. G. (2011). A European daily high-resolution observational gridded data set of sea level pressure. *Journal of Geophysical Research: Atmospheres (1984–2012)*, 116(D11).
- Blair, D. (1998). The Kirchhofer technique of synoptic typing revisited. *International journal of climatology*, 18(14), 1625-1635.
- Chen, D. (2000). A monthly circulation climatology for Sweden and its application to a winter temperature case study. *International Journal of Climatology*, 20(10), 1067-1076.
- Dee, D. P., Uppala, S. M., Simmons, A. J., Berrisford, P., Poli, P., Kobayashi, S., Andrae, U., Balmaseda, M. A., Balsamo, G., Bauer, P., Bechtold, P., Beljaars, A. C. M., van de Berg, L., Bidlot, J., Bormann, N., Delsol, C., Dragani, R., Fuentes, M., Geer, A. J., Haimberger, L., Healy, S. B., Hersbach, H., Hólm, E. V., Isaksen, L., Kållberg, P., Köhler, M., Matricardi, M., McNally, A. P., Monge-Sanz, B. M., Morcrette, J.-J., Park, B.-K., Peubey, C., de Rosnay, P., Tavolato, C., Thépaut, J.-N. and Vitart, F. (2011), The ERA-Interim reanalysis: configuration and performance of the data assimilation system. *Q.J.R. Meteorol. Soc.*, 137: 553–597. doi: 10.1002/qj.828
- Esteban, P., Martin-Vide, J., & Mases, M. (2006). Daily atmospheric circulation catalogue for Western Europe using multivariate techniques. *International journal of climatology*, 26(11), 1501-1515.
- Fleig, A. K., Tallaksen, L. M., Hisdal, H., Stahl, K., & Hannah, D. M. (2010). Inter-comparison of weather and circulation type classifications for hydrological drought development. *Physics and Chemistry of the Earth, Parts A/B/C*, 35(9), 507-515.
- Furevik, T., Bentsen, M., Drange, H., Kindem, I. K. T., Kvamstø, N. G., & Sorteberg, A. (2003). Description and evaluation of the Bergen climate model: ARPEGE coupled with MICOM. *Climate Dynamics*, 21(1), 27-51.

- Huth, R. (2000). A circulation classification scheme applicable in GCM studies. *Theoretical and applied climatology*, 67(1), 1-18.
- Huth, R. (2001). Disaggregating climatic trends by classification of circulation patterns. *International Journal of Climatology*, 21(2), 135-153.
- Huth, R., Beck, C., Philipp, A., Demuzere, M., Ustrnul, Z., Cahynová, M., Kyselý, J., & Tveito, O. E. (2008). Classifications of atmospheric circulation patterns. *Annals of the New York Academy of Sciences*, 1146(1), 105-152.
- Kirchhofer, W. (1974). Classification of European 500 mb patterns. *Swiss Meteorological Institute*.
- Kohonen, T. (1990). The self-organizing map. *Proceedings of the IEEE*, 78(9), 1464-1480.
- Landgren, O.A., Skaugen, T.E., Haugen, J.E, Førland, E.J. (2012), An evaluation of temperature and precipitation from global and regional climate models over Scandinavia, *met.no Report*, no. 21a
- Linderson, M.-L. (2001), Objective classification of atmospheric circulation over southern Scandinavia. *Int. J. Climatol.*, 21: 155–169. doi: 10.1002/joc.604
- Lund, I. A. (1963). Map-pattern classification by statistical methods. *Journal of Applied Meteorology*, 2(1), 56-65.
- Philipp, A., Della-Marta, P. M., Jacobeit, J., Fereday, D. R., Jones, P. D., Moberg, A., & Wanner, H. (2007). Long-term variability of daily North Atlantic-European pressure patterns since 1850 classified by simulated annealing clustering. *Journal of Climate*, 20(16), 4065-4095.
- Philipp, A., Bartholy, J., Beck, C., Erpicum, M., Esteban, P., Fettweis, X., Huth, R., James, P., Jourdain, S., Kreienkamp, F., Krennert, T., Lykoudis, S., Michalides, S. C., Pianko-Kluczynska, K., Post, P., Álvarez, D. R., Schiemann, R., Spekat, A. & Tymvios, F. S. (2010). Cost733cat—A database of weather and circulation type classifications. *Physics and Chemistry of the Earth, Parts A/B/C*, 35(9), 360-373.
- Plavcová, E., & Kyselý, J. (2013). Projected evolution of circulation types and their temperatures over Central Europe in climate models. *Theoretical and Applied Climatology*, 1-10.
- Tveito, O. E. (2007). Spatial distribution of winter temperatures in Norway related to topography and large-scale atmospheric circulation. *IAHS Publication*, (309), 186-194.
- Tveito, O. E. (2010). An assessment of circulation type classifications for precipitation distribution in Norway. *Physics and Chemistry of the Earth, Parts A/B/C*, 35(9), 395-402.
- Uppala, S. M., Kållberg, P. W., Simmons, A. J., Andrae, U., Bechtold, V. D. C., Fiorino, M., Gibson, J. K., Haseler, J., Hernandez, A., Kelly, G. A., Li, X., Onogi, K., Saarinen, S., Sokka, N., Allan, R. P., Andersson, E., Arpe, K., Balmaseda, M. A., Beljaars, A. C. M., Berg, L. V. D., Bidlot, J., Bormann, N., Caires, S., Chevallier, F., Dethof, A., Dragosavac, M., Fisher, M., Fuentes, M., Hagemann, S., Hólm, E., Hoskins, B. J., Isaksen, L., Janssen, P. A. E. M., Jenne, R., McNally, A. P., Mahfouf, J.-F., Morcrette, J.-J., Rayner, N. A., Saunders, R. W., Simon, P., Sterl, A., Trenberth, K. E., Untch, A., Vasiljevic, D., Viterbo, P. and Woollen, J. (2005), The ERA-40 re-analysis. *Q.J.R. Meteorol. Soc.*, 131: 2961–3012. doi: 10.1256/qj.04.176

## Appendix

A few extra figures are included in order to illustrate some points of discussion.

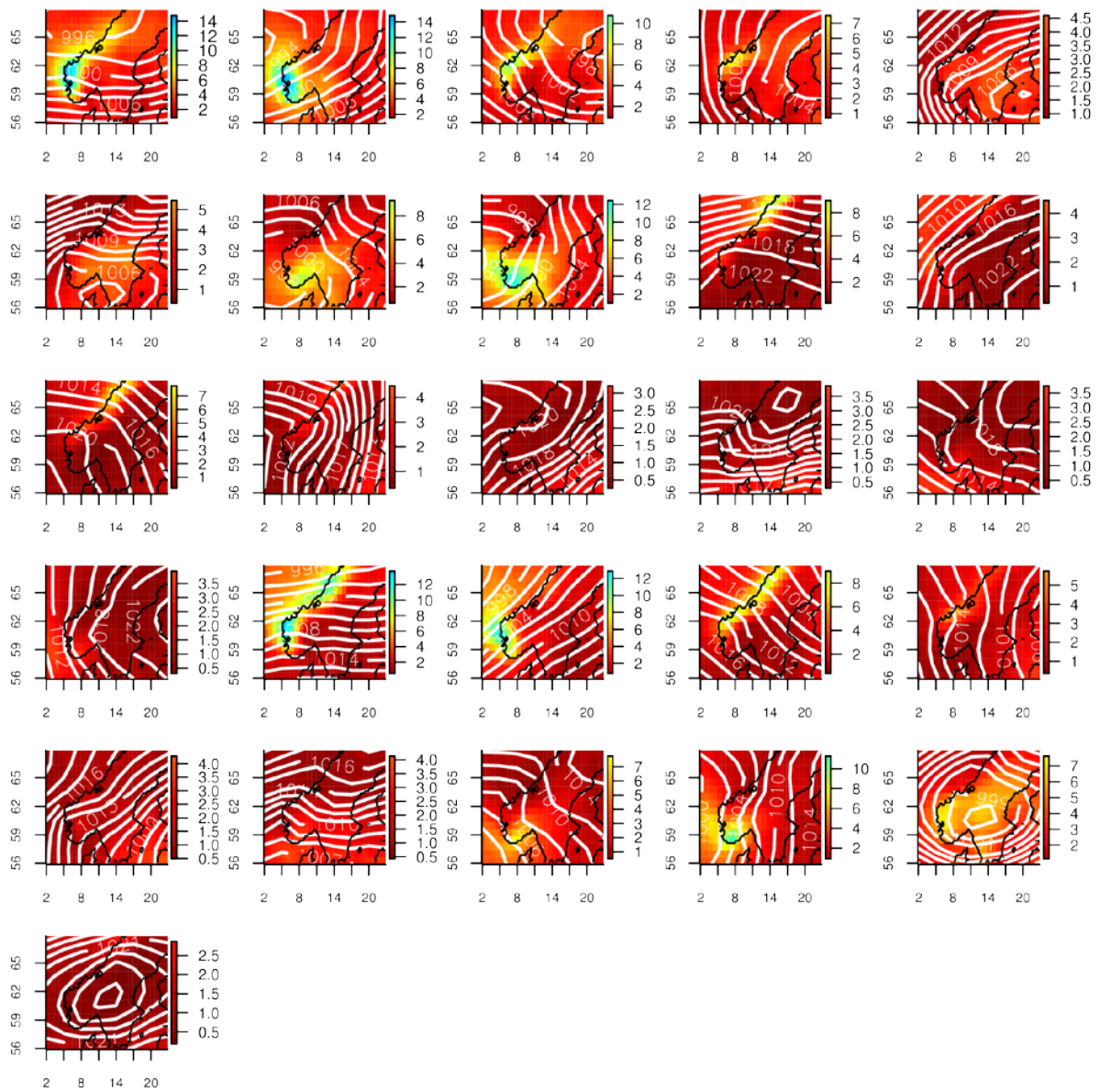


Fig. A.1: Grosswetterlagen method using 26 classes (GWT26). Similar to Fig. 4.1a but with a higher number of classes. The corresponding annual cycle is presented in Fig. A.2.

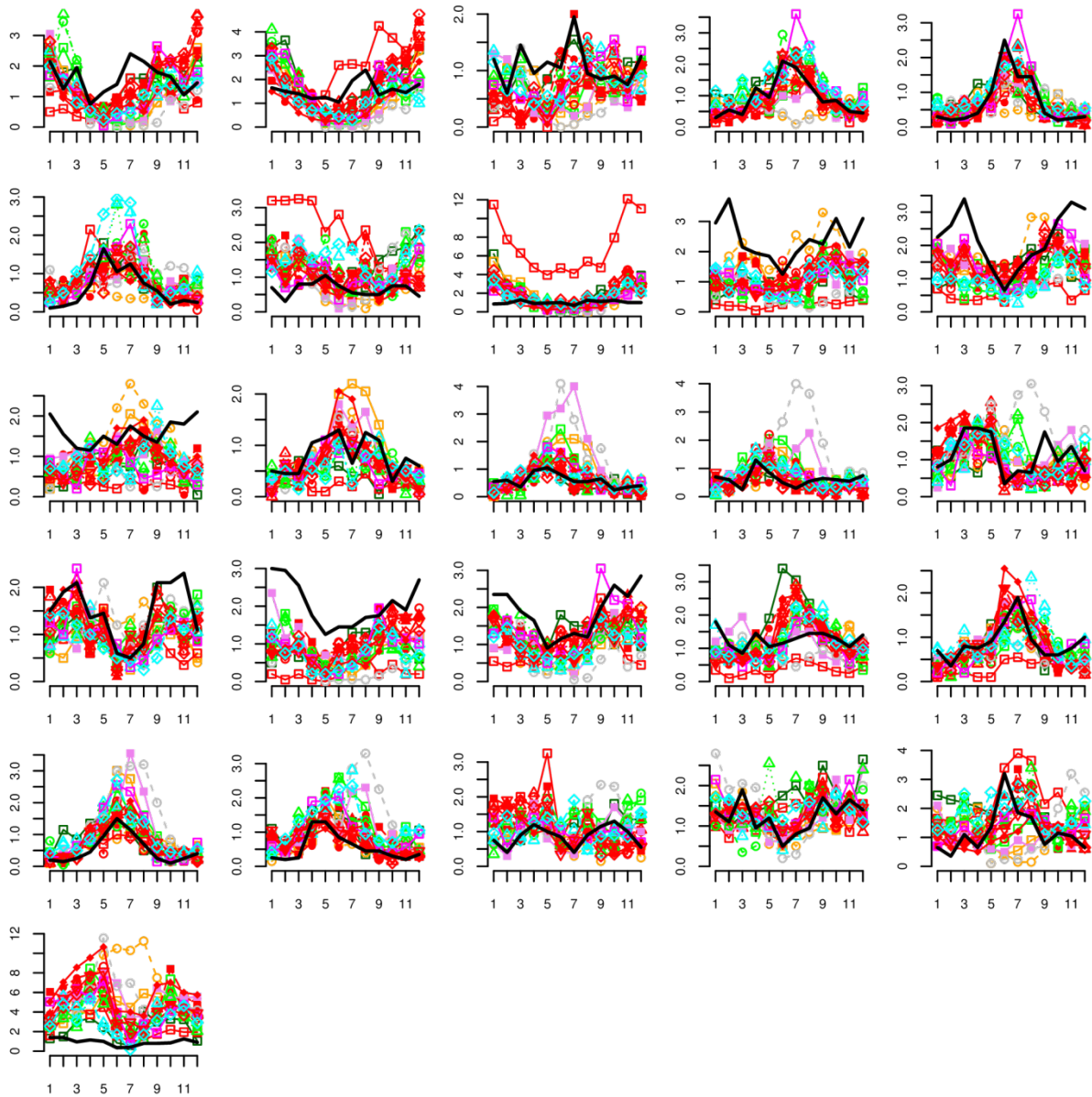


Fig. A.2: Annual distribution of classes for Grosswetterlagen method using 26 classes (GWT26). Similar to Fig. 4.2a but with a higher number of classes. The corresponding classes are presented in Fig. A.1.

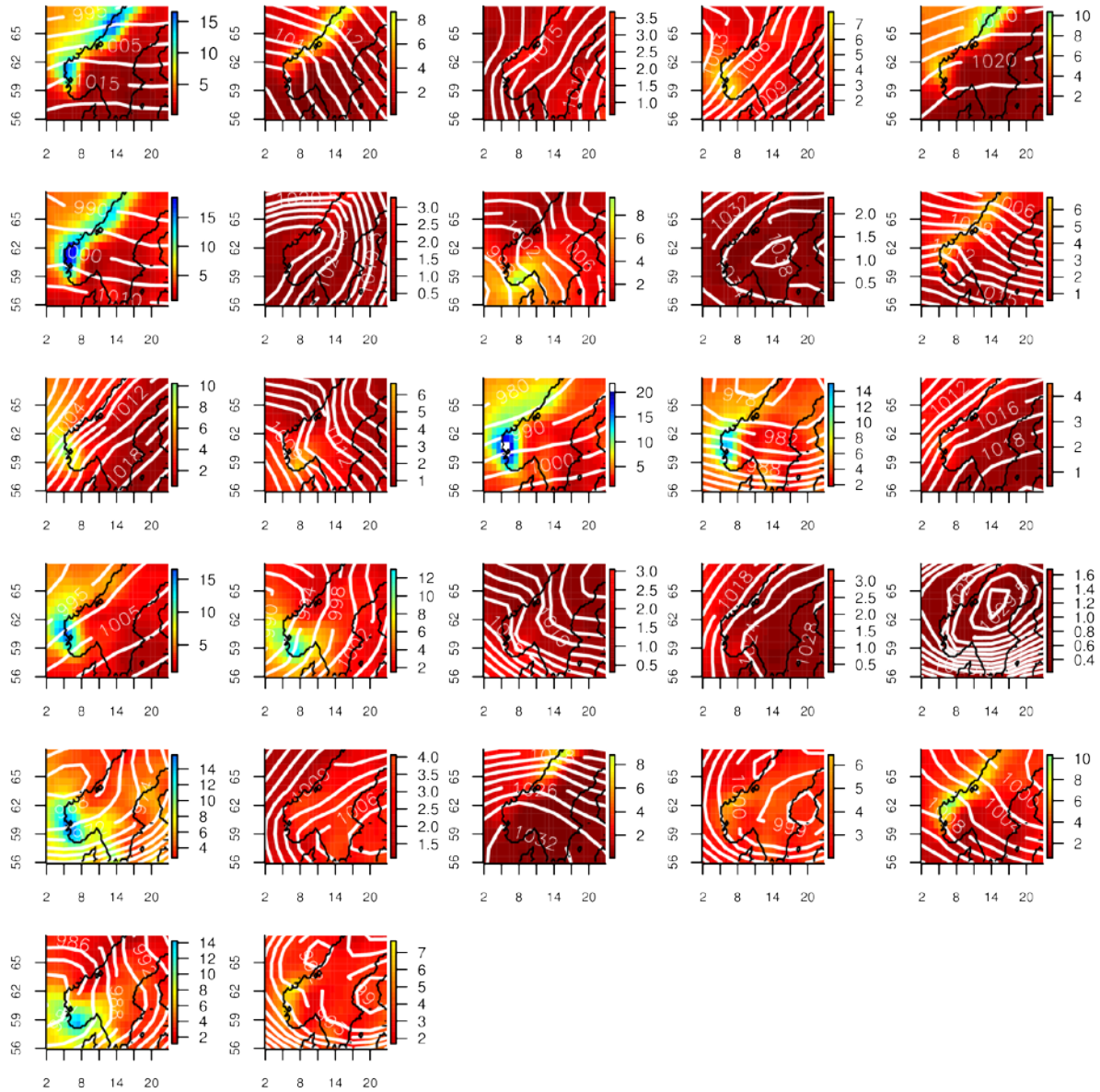


Fig. A.3: SANDRA method using 27 classes (SAN27). Similar to Fig. 4.1b but with a higher number of classes. The corresponding annual cycle is presented in Fig. A.4.

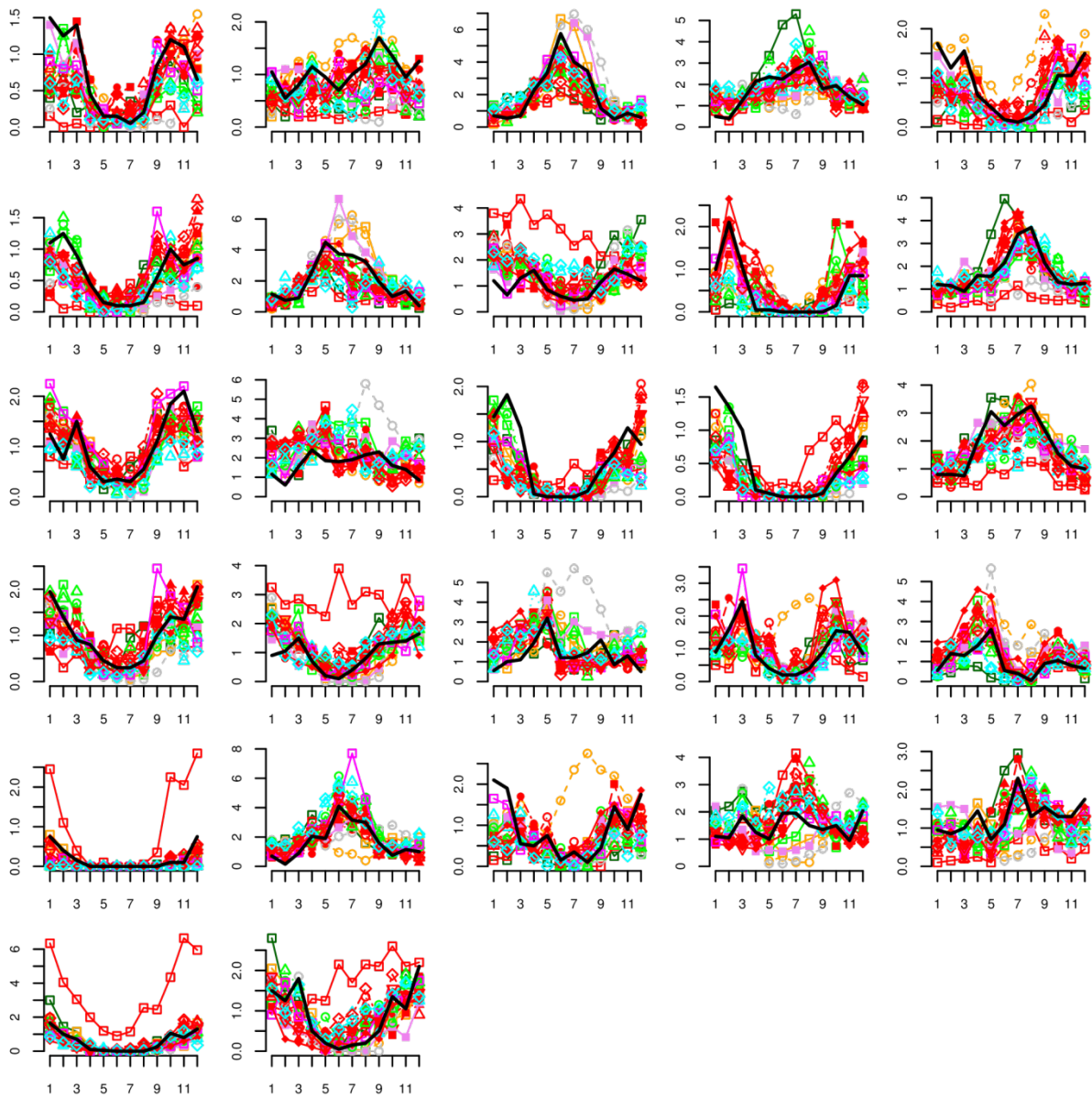


Fig. A.4: Annual distribution of classes for SANDRA using 27 classes (SAN27). Similar to Fig. 4.2b but with a higher number of classes. The corresponding classes are presented in Fig. A.3.

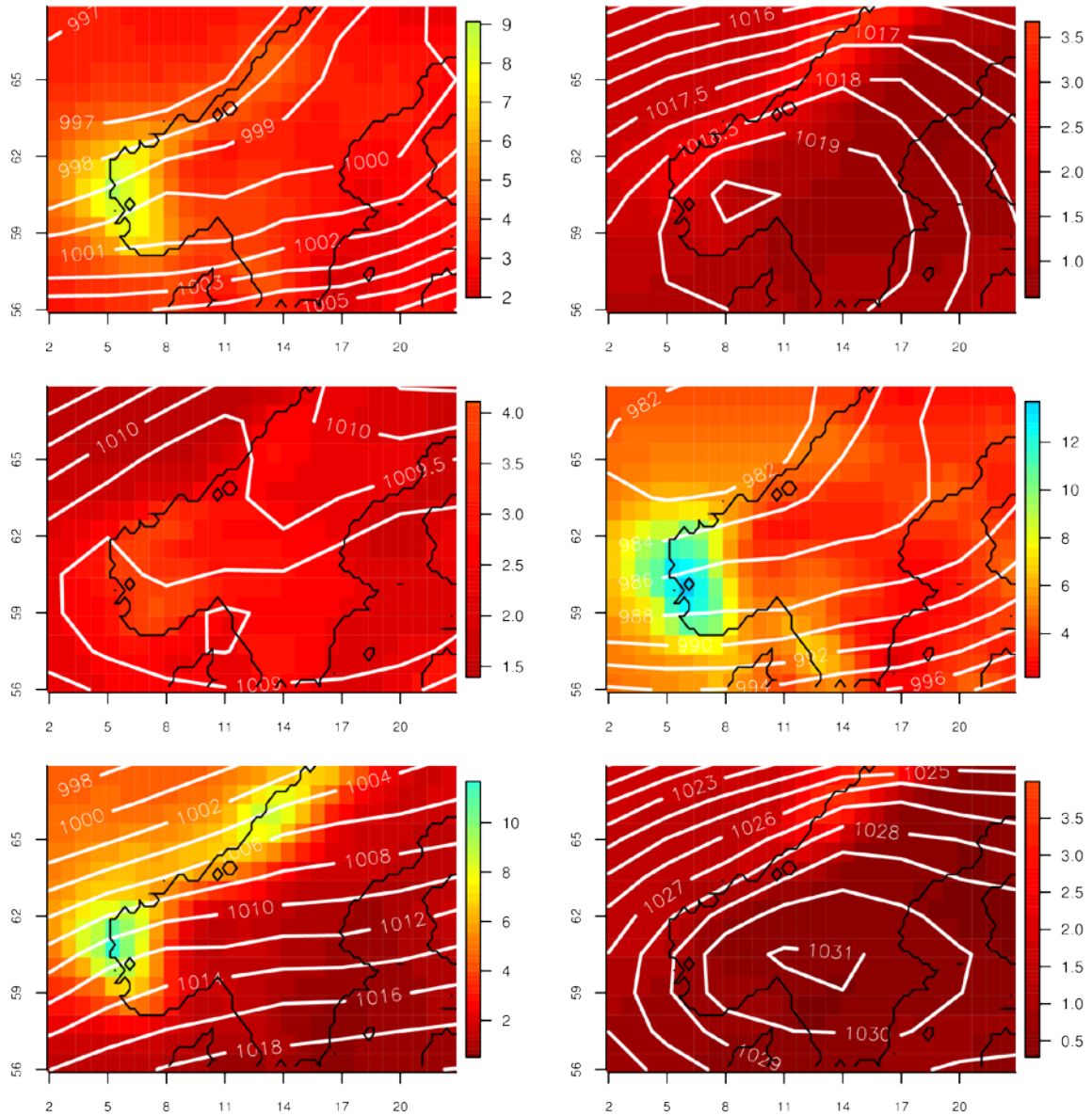


Fig. A.5: Classes produced by Self-Organizing Maps using 6 classes (SOM06). The results are very similar to those from SAN06 (Fig. 4.1b).

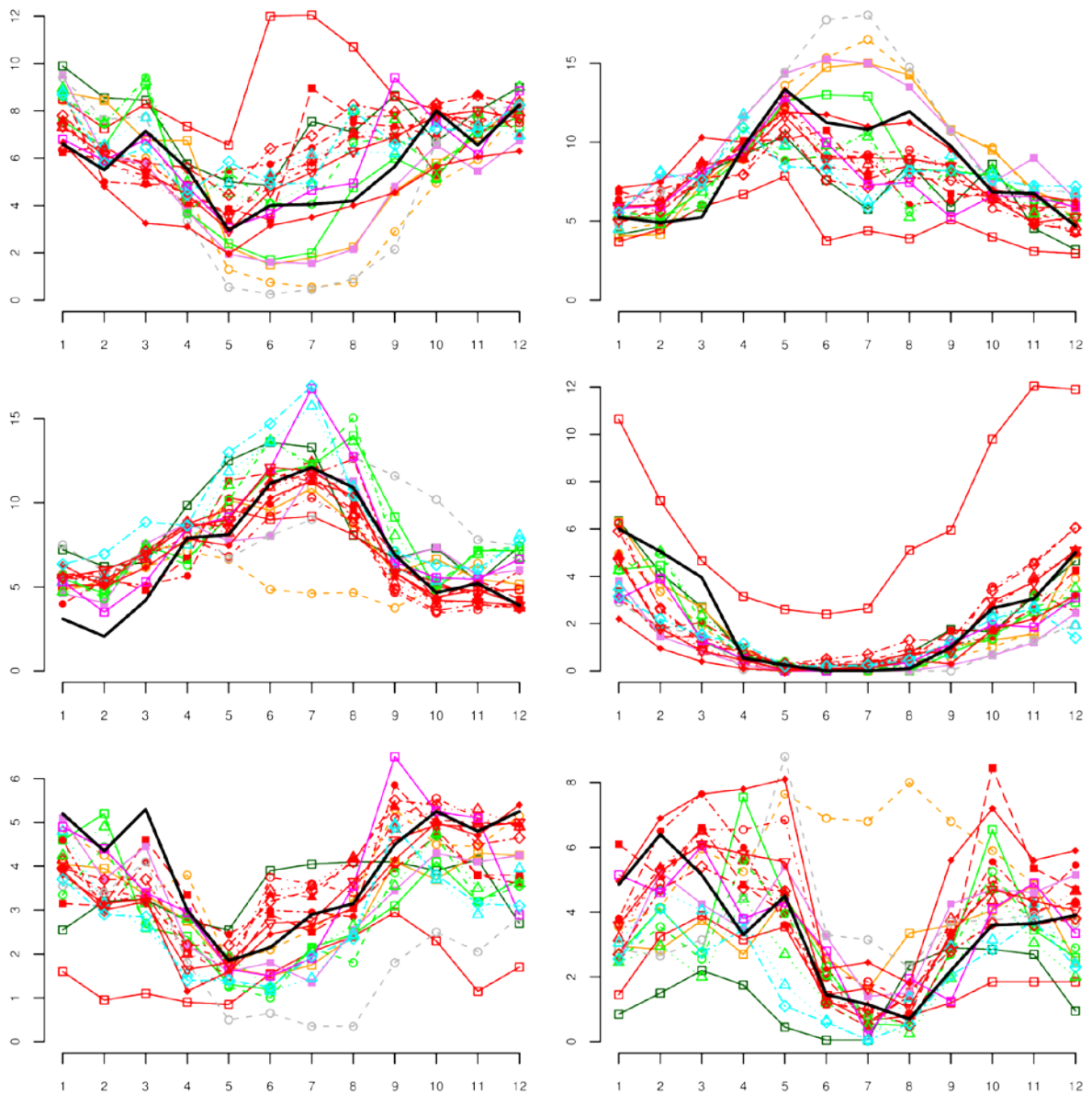


Fig. A.6: Self-Organizing Maps method using 6 classes (SOM06). Annual distribution of classes from Fig. A.5. The results are very similar to those from SAN06 (Fig. 4.1b).

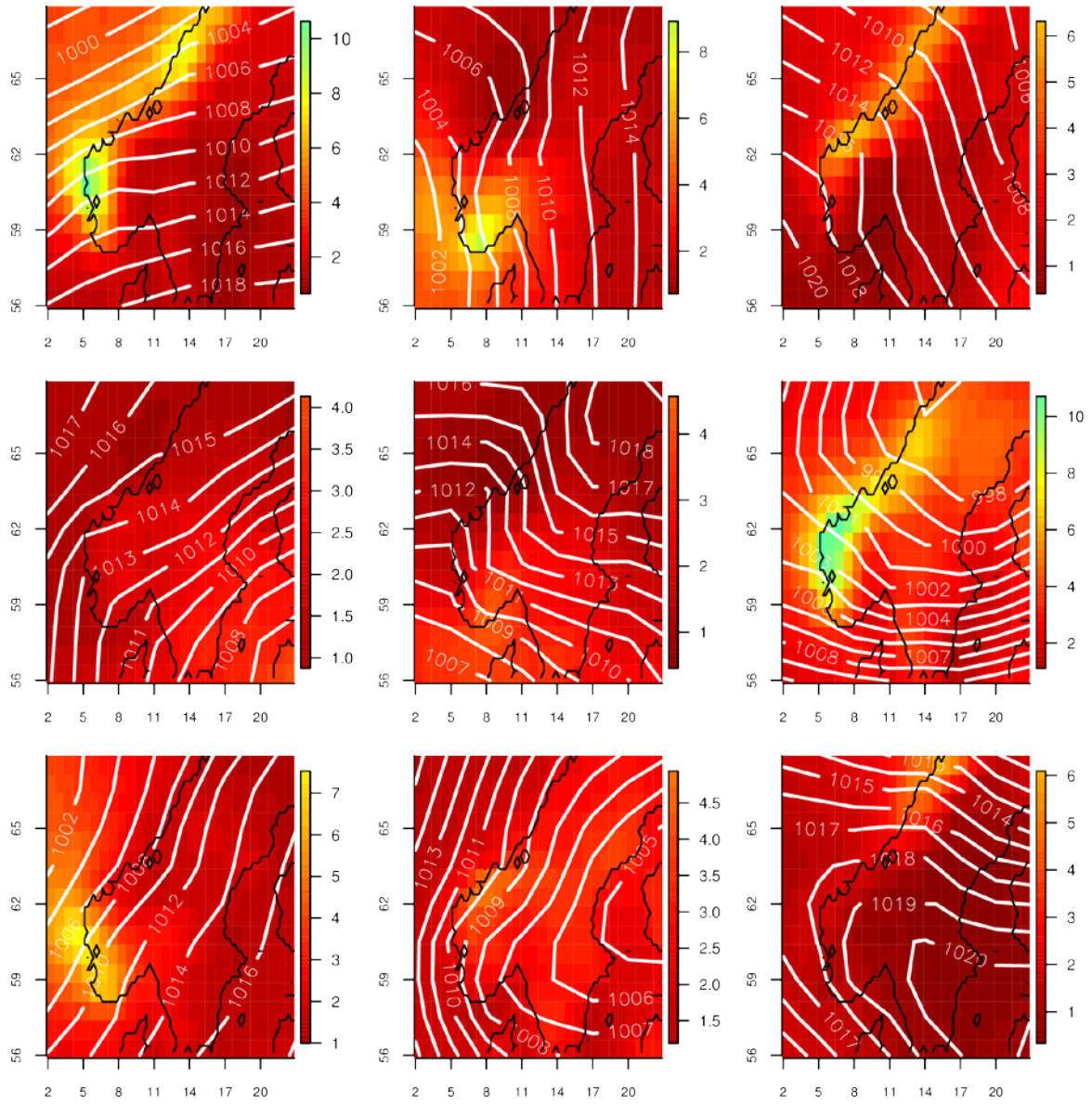


Fig. A.7: Lund method using 9 classes (LND09). The corresponding annual cycle is presented in Fig. A.8.

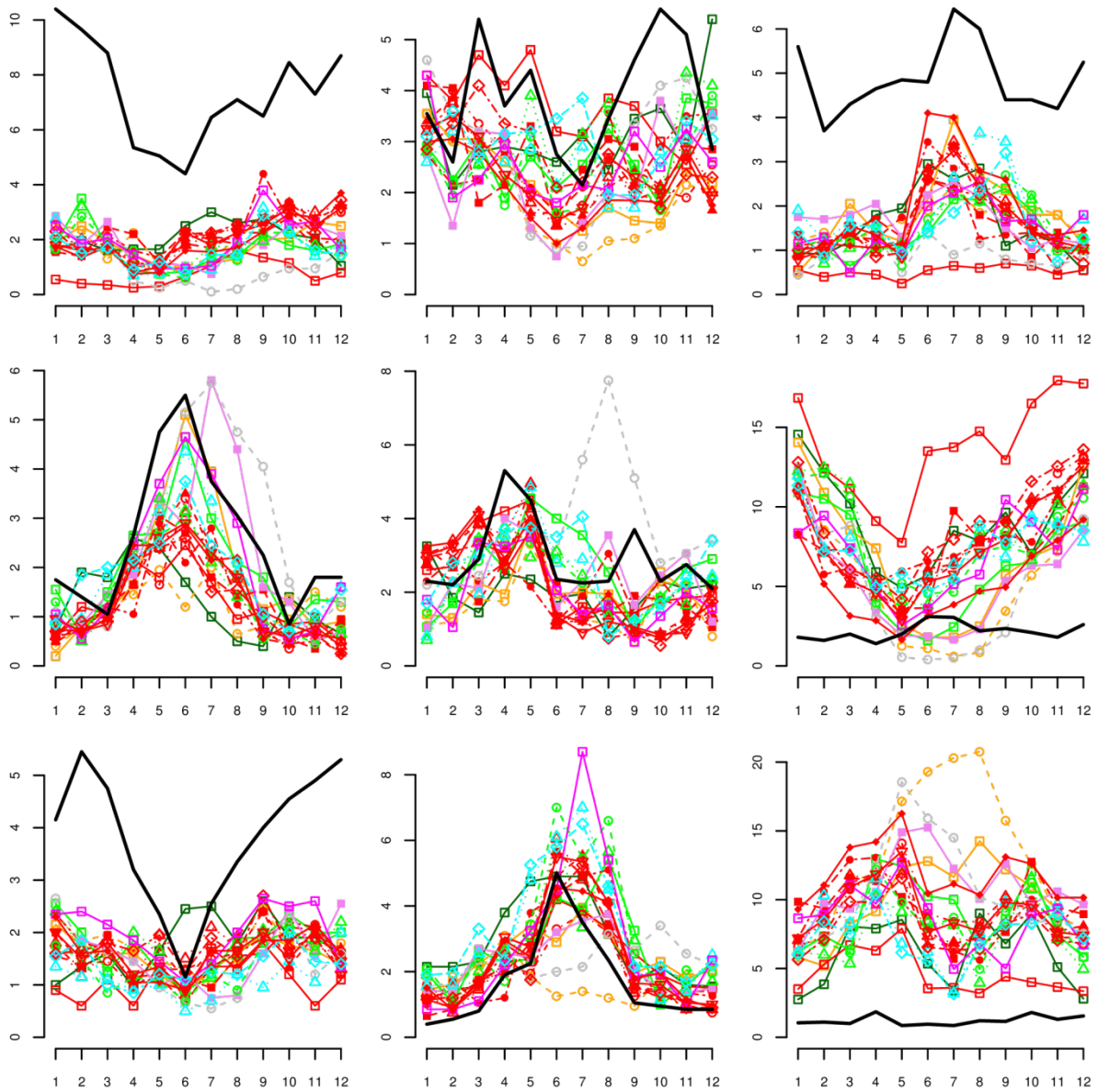


Fig. A.8: Lund method using 9 classes (LND09). Annual distribution of classes from Fig. A.7.

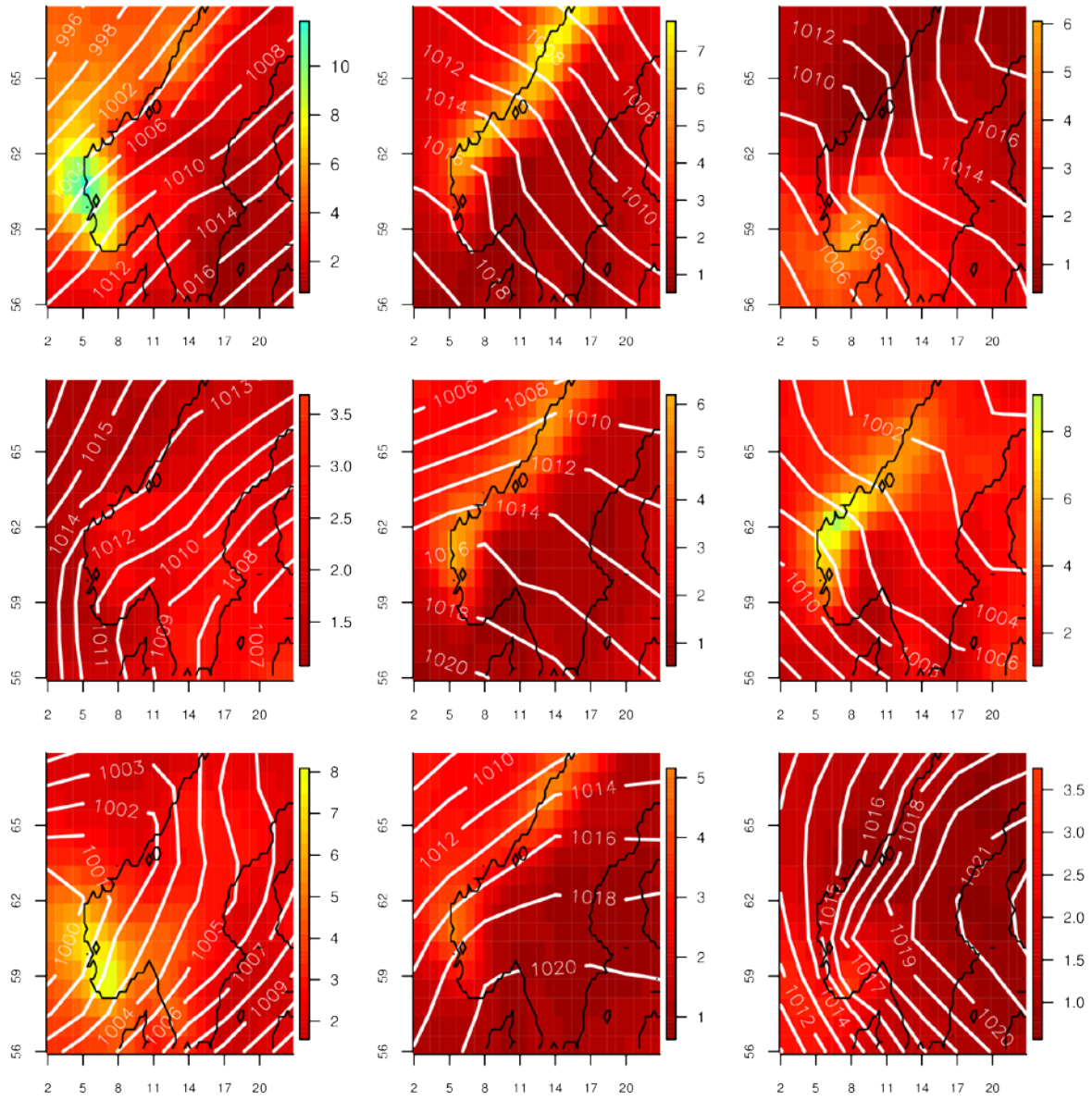


Fig. A.9: Kirchofer method using 9 classes (KIR09). The corresponding annual cycle is presented in Fig. A.10.

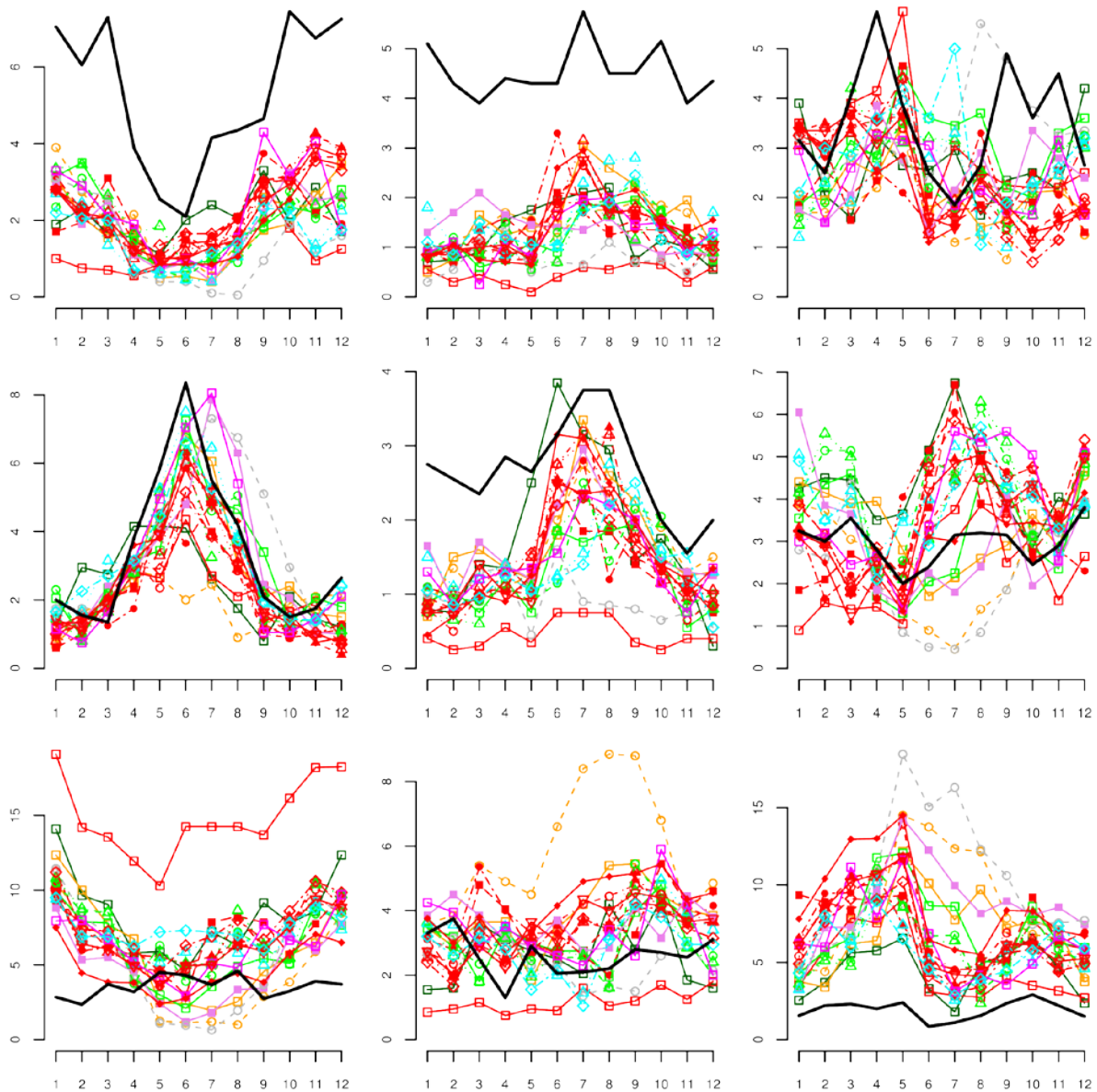


Fig. A.10: Kirchofer method using 9 classes (KIR09). Annual distribution of classes from Fig. A.9.

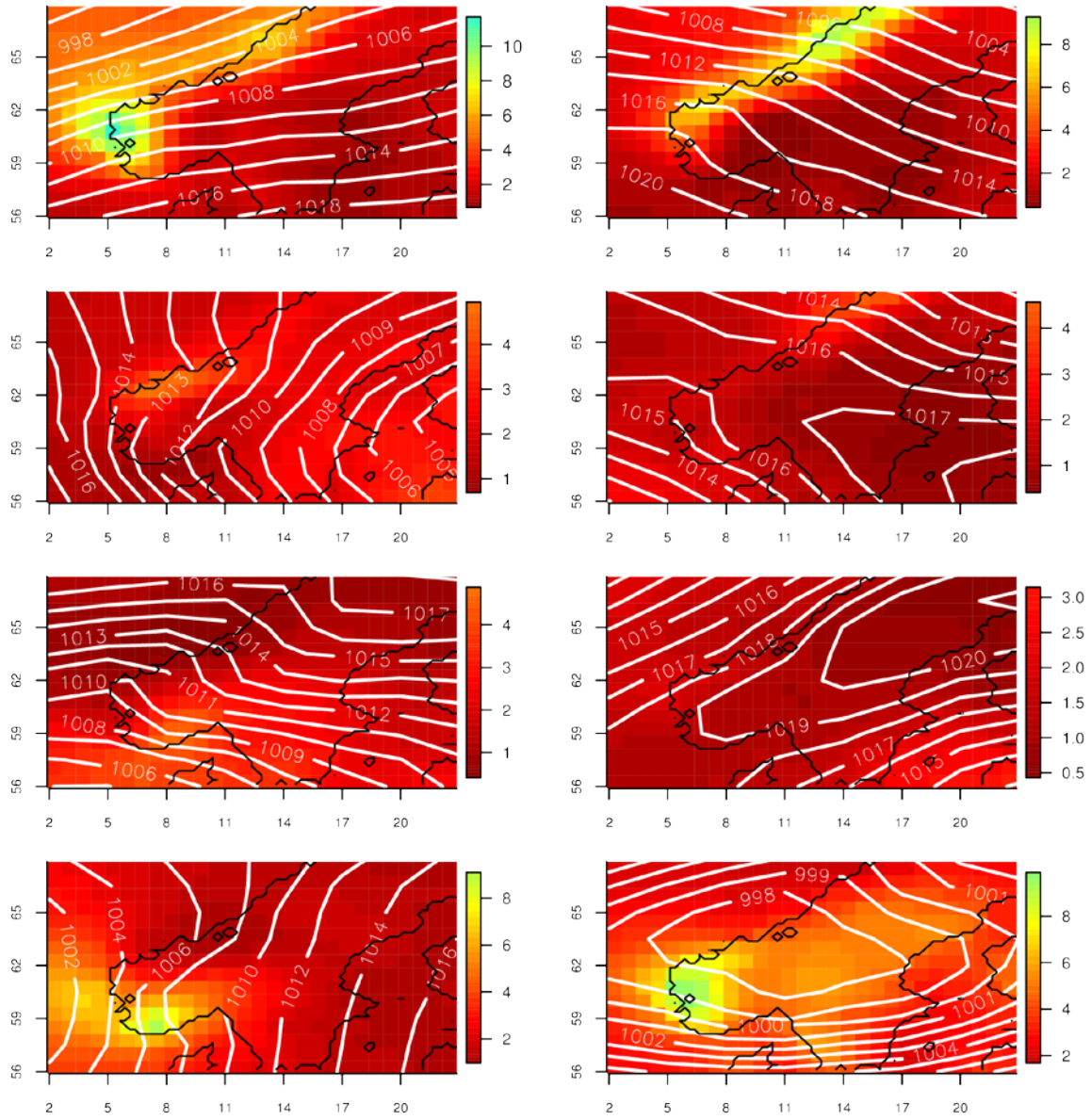


Fig. A.11: PXX method using 8 classes (PXX08). The corresponding annual cycle is presented in Fig. A.12.

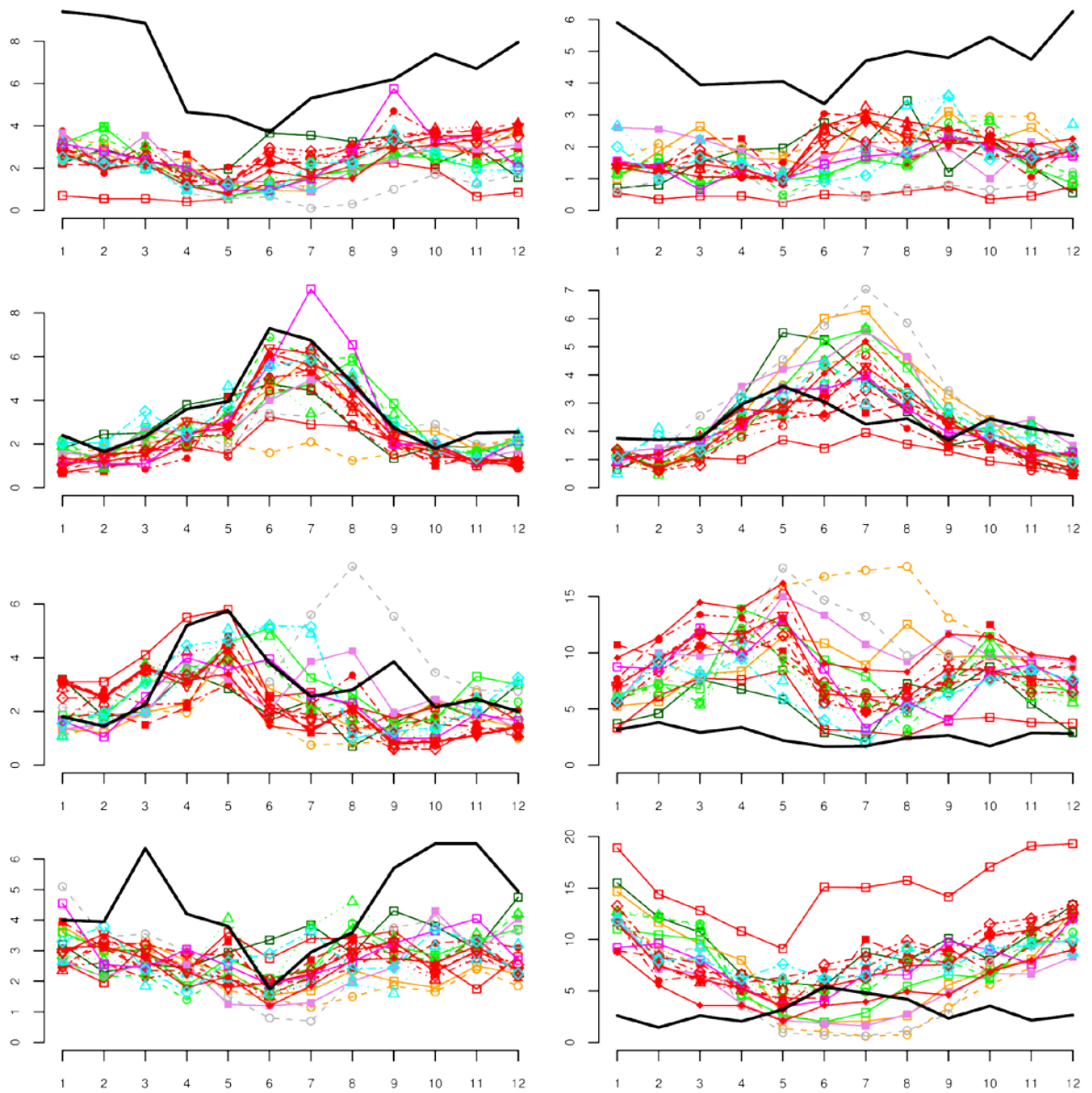


Fig. A.12: PXX method using 8 classes (PXX08). Annual distribution of classes from Fig. A.11.